3460, 3340, 3090, 3040, 2980, 1650, 1510, 1450, 1385, 1365, 1215, 1070, 985, 915, 700 cm^{-1}; EI mass spectrum, *m/e* (rel intensity) 275 (11, M^+), 244 (22), 234 (48), 216 (30), 190 (8), 145 (21), 131 (38), 91 (100), 72 (89), 60 (29), 41 (35). Anal. Calcd for $C_{17}H_{25}NO_2$: C, 74.14; H, 9.15; N, 5.09. Found: C, 74.42; H, 8.99; N, 5.18] and **12r** [3.2% yield; mp 94.5-95.5 °C from *n*-hexane/EtOAc; $[\alpha]^{25}_D$ -7.02 (*c* 5.34, $CHCl_3$); ^1H NMR δ 0.63 (d, J = 7 Hz, 3 H), 0.70 (d, J = 7 Hz, 3 H), 1.43-1.80 (m, 1 H), 2.10-2.45 (m, 3 H), 2.61 (br s, OH, 1 H), 2.70-3.14 (m, 2 H), 3.40-3.73 (m, 3 H), 4.90-5.25 (m, 2 H), 5.25-5.50 (m, NH, 1 H), 5.54-6.07 (m, 1 H), 7.0-7.5 (m, 5 H); IR (CCl_4) 3450, 3090, 3040, 3010, 2980, 1650, 1595, 1500, 1450, 1375, 1355, 1240, 1070, 985, 910, 800, 695 cm^{-1}; EI mass spectrum *m/e* (rel intensity) 275 (7, M^+), 244 (20), 234 (46), 216 (11), 190 (8), 145 (18), 131 (38), 91 (97), 72 (100), 60 (36), 43 (30), 41 (45). Anal. Calcd for $C_{17}H_{25}NO_2$: C, 74.14; H, 9.15; N, 5.09. Found: C, 74.19; H, 9.06; N, 4.97]. A recrystallized sample of **12s** was subjected to single-crystal X-ray diffraction analysis. Compound **12s** crystallizes from *n*-hexane/EtOAc in the orthorhombic space group, $P2_12_12_1$. The crystal data at 140 K are as follows: a = 5.054 (2) Å, b = 20.342 (8) Å, c = 16.170 (6) Å; ρ(calcd) = 1.10 g cm^{-3} for Z = 4; 2θ(max) = 50°; 2466 reflections with $F > 6\sigma(|F|)$ used, Mo Kα (graphite (λ = 0.71069 Å), and ω scan, 20° min^{-1}; R = 0.045. SHELXTL programs were used on a DGC Eclipse S/230 computer.

Acknowledgment is made to the Committee on Research of the University of California, Davis, the Cancer Research Coordinating Committee, University of California, and to the donors of the Petroleum Research Fund, administered by the American Chemical Society, for the support of this research. We gratefully acknowledge IBM Instruments for the donation of an LC/9533 ternary high-pressure liquid chromatography system.

Registry No. 1a, 93684-28-7; **1b**, 93684-29-8; **1c**, 93684-30-1; **1d**, 93684-31-2; **1e**, 93684-32-3; **1f**, 93684-33-4; **1g**, 93714-43-3; **1h**, 93684-34-5; **2a**, 93684-35-6; **2b**, 93684-36-7; **2c**, 93684-37-8; **2d**, 93684-38-9; **2e**, 93684-39-0; **2f**, 93684-40-3; **2g**, 93684-41-4; **2h**, 88362-53-2; **4c**, 93780-03-1; **4h**, 63527-49-1; **5a**, 93684-42-5; **5b**, 93684-43-6; **5c**, 93684-44-7; **5d**, 93684-45-8; **5e**, 93684-46-9; **5f**, 93684-47-0; **5g**, 93684-48-1; **5h**, 88362-45-2; **6a**, 93684-50-5; **6b**, 93684-52-7; **6c**, 93684-54-9; **6d**, 93684-56-1; **6e**, 93684-58-3; **6f**, 93684-60-7; **6g**, 93684-62-9; **6h**, 88362-48-5; **7a**, 93684-63-0; **7b**, 93684-64-1; **7c**, 93684-65-2; **7d**, 93684-66-3; **7e**, 93684-67-4; **7f**, 93684-68-5; **7g**, 93684-69-6; **7h**, 88362-54-3; **8**, 93684-70-9; **10c**, 93780-04-2; **10h**, 20626-61-3; **11r**, 93714-44-4; **11s**, 93714-45-5; **12s**, 93684-71-0; **12r**, 93780-05-3; 2-amino-1-butanol, 13054-87-0; β-aminobenzenepropanol, 1795-98-8; L-valinol, 2026-48-4; (*S*)-2-amino-3,3-dimethyl-1-butanol, 93684-72-1; β-aminobenzeneethanol, 71006-16-1; benzenepropionic acid, 501-52-0; propionic acid, 79-09-4; β,β-dimethylbenzenepropionic acid, 1010-48-6; ethyl propanimidate hydrochloride, 40546-35-8; isobutyric acid, 79-31-2; (*S*)-(-)-4,5-dihydro-2,4-bis(1-methylethyl)oxazole, 93684-73-2; (*S*)-(-)-4,5-dihydro-2,4-bis(1-methylethyl)-3-(2-propenyl)-oxazolinium 4-methylbenzenesulfonate, 93684-75-4.

Supplementary Material Available: A stereoplot of **12s**, listings of bond distances, bond angles, hydrogen atom coordinates, isotropic, and anisotropic temperature factors, and observed and calculated structure factors (18 pages). Ordering information is given on any current masthead page.

Host-Guest Complexation. 34. Bridged Hemispherands[1,2]

George M. Lein and Donald J. Cram*

Contribution from the Department of Chemistry and Biochemistry, University of California at Los Angeles, Los Angeles, California 90024. *Received July 13, 1984*

Abstract: The synthesis and binding properties of 11 new hemispherands (**2-12**) are reported, 7 of which contain extra bridges that help preorganize the systems for complexation. These hosts are composed of the following units bonded to one another in 18-membered ring systems: 2,6-disubstituted 4-methylanisyl; 2,6-disubstituted 4-methylphenol; 2,6-disubstituted 4-methyl-1-(allyloxy)benzene; 6-aryl-substituted 4-methyl-1-methoxybenzene; 2,6-disubstituted pyridine; and pyridine oxide, ethylene, methylene, and oxygen. Association constants (K_a) between host and guest to give complexes were determined by extracting picrate salts (guests) from D_2O into $CDCl_3$ in the absence and presence of hosts at 25 °C. The rates of extraction were essentially instantaneous. The free energies of complexation for the 11 new hosts with picrate salts of Li^+, Na^+, K^+, Rb^+, Cs^+, NH_4^+, $CH_3NH_3^+$, and t-$BuNH_3^+$ were determined. These $-\Delta G°$ values ranged from a high of 14.6 kcal mol^{-1} to a low of ~2.8 kcal mol^{-1}. Interesting structural recognition factors ($K_a^G/K_a^{G'}$) for a host distinguishing between two similar guests (G and G') are Na^+/Li^+ = 9500 (**8**), Na^+/K^+ = 14 (**9**), K^+/Na^+ = 9 (**7**), K^+/Rb^+ = 54 (**11**), Rb^+/Cs^+ = 55 (**6**), $NH_4^+/CH_3NH_3^+$ = 31 (**10**), and $CH_3NH_3^+/t$-$BuNH_3^+$ = 40 (**10**). The strongest binding host for all ions is **12**, which gave a $-\Delta G°_{av}$ for the eight ions of 12.5 kcal mol^{-1}. It is also the most rigid and least discriminating of the hosts. Correlations between the structures of the complexes and their free energies of binding are interpreted in terms of the principles of complementarity and preorganization.

Hemispherands are host compounds, at least half of whose binding sites are conformationally organized for binding during their synthesis, rather than during their complexation. In other words, hemispherands are at least half preorganized for binding. The synthesis and complexing properties have been previously reported for several members of this class of hosts for which compound **1** is prototypical.[3] This compound is composed of three self-organizing anisyl units combined with three additional

Chart I

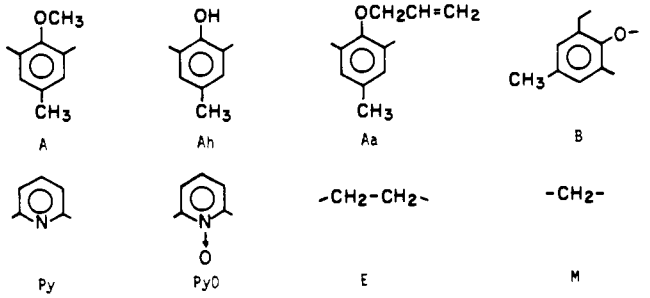

CH_2OCH_2 binding sites. Other hemispherands have been reported that contain four anisyl units[4] or anisyl and cyclic urea units.[5,6]

(1) We warmly thank the Division of Basic Energy Sciences, Department of Energy (DOE EY 76-S-03-0034, P.A. 218), for a contract that supported this research.

(2) The binding free energies of compounds **1**, **4**, and **8** have appeared in a communication: Cram, D. J.; Dicker, I. B.; Lein, G. M.; Knobler, C. B.; Trueblood, K. N. *J. Am. Chem. Soc.* **1982**, *104*, 6827-6828.

(3) Koenig, K.; Lein, G. M.; Stuckler, P.; Kaneda, T.; Cram, D. J. *J. Am. Chem. Soc.* **1979**, *101*, 3553-3566.

0002-7863/85/1507-0448$01.50/0

Here we report the synthesis and binding properties of new hosts **2–12**, each of which contains a terphenyl molecular module attached to three binding OR groups or two OR and one OH groups. Each host is part of an 18-membered ring system containing three additional binding sites. Seven of the 11 new cycles contain an additional bridge which increases the degree of preorganization of the hosts. With certain complexing partners, preorganization enhances, and with others, preorganization inhibits complexation. In some systems the extra bridge also contains extra binding sites. These compounds were designed and prepared to extend our correlations of structure with binding properties toward alkali metal, ammonium, and alkylammonium ions.[7,8]

Because of the complexity of the systematic names of these compounds, they are conveniently referred to in-line formulas in which letters identify the units, and their orders of appearance in the line formulas identify their bonding patterns. Chart I identifies the letters with the structures of the units. Chart II provides the structures formulas of hosts **1–12** and their associated line formulas.

Results

Syntheses. In a synthesis of **1** superior to one that has been reported,[3] HAhAhAhH (**13**) was methylated with 1 M equiv of K_2CO_3 and excess CH_3I in acetone to give HAhAAhH (**17**), which without characterization was hydroxymethylated with KOH–$(CH_2O)_n$–*i*-PrOH–H_2O to provide HOMAhAAhMOH (**18**, 49% based on **13**). Methylation of the two phenolic hydroxyls of this compound ($(CH_3)_2SO_4$–K_2CO_3–acetone) gave HOMAAAMOH (**16**, 96%). Similarly, HAhAhAhH (**13**) was allylated with $CH_2{=}CHCH_2Br$–K_2CO_3 to provide HAhAaAhH (**19**), which in turn was hydroxymethylated to give HOMAhAaAhMOH (**20**, 54% based on **13**). Methylation of the two phenolic hydroxyls of this tetrol with $(CH_3)_2SO_4$–THF–NaOH led to HOMAAaAMOH (**21**, 63%).

Key intermediate HOMAhAaAhMOH (**20**) was bridged under high dilution conditions in $(CH_2)_4O$–2% H_2O–NaOH with $O(CH_2CH_2OTs)_2$ to give HOMB[Aa][EOE]BMOH (**22**, 51%), with $Br(CH_2)_3Br$–KI to produce HOMB[Aa][M_3]BMOH (**23**, 42%), with $Br(CH_2)_4Br$–KI to provide HOMB[Aa][M_4]BMOH (**24**, 49%), with $Br(CH_2)_5Br$–KI to give HOMB[Aa][M_5]BMOH (**25**, 51%), and with $BrCH_2PyCH_2Br$[9] to produce HOMB[Aa][MPyM]BMOH (**26**, 69%). The greater acidity of the phenolic over the benzylic hydroxyl groups of HOMAhAaAhMOH (**20**) allowed the phenoxide anions to dominante these base-catalyzed substitution reactions, leaving the hydroxymethylene groups intact. The five cyclic diols **22–26** were converted to their corresponding dibromides, **27–31**, by treatment with PBr_3–C_6H_6 in 50–79% yields. Likewise, open-chain diols HOMAAAMOH (**16**) and HOMAAaAMOH (**21**) were converted to BrMAAAMBr (**32**, 63%) and BrMAAaAMBr (**33**, 59%), respectively.

Macrocyclic hosts **1**, **2**, **4**, **6**, and **9–12** were prepared by the slow addition of a solution of the appropriate dibromide (**32**, **33**, **27**, **29**, **30**, or **31**) mixed in THF with either diethylene glycol or pyrido-2,6-dimethanol[10] to a refluxing suspension of NaH–THF using a reflux-return high-dilution apparatus. The products were produced in the following yields: A(AMOE)$_2$O (**1**), 49%; Aa(AMOE)$_2$O (**2**), 33%; A(AMOM)$_2$Py (**4**), 27%; B[Aa][EOE][(MOE)$_2$O]B (**6**), 21%; B[Aa][M_4][(MOE)$_2$O]B (**9**), 33%; B[Aa][M_5][(MOE)$_2$O]B (**10**), 25%; B[Aa][EOE][(MOM)$_2$Py]B (**11**), 21%; and B[Aa][MPyM][(MOE)$_2$O]B (**12**, 4%). The yield of A(AMOE)$_2$O (**1**) produced by this method (49%) was superior to the 35% obtained through the reaction of HOMAAAMOH (**16**) with $O(CH_2CH_2OTs)_2$.[3] Attempts to prepare B[Aa][M_3][(MOE)$_2$O]B from BrMB[Aa][M_3]BMBr (**28**) and diethylene glycol or from HOMB[Aa][M_3]BMOH (**23**) and $O(CH_2CH_2OTs)_2$ failed to give isolable amounts of host. Serious attempts to obtain the 15-membered host A(AMO)$_2$E by the reaction of BrMAAAMBr (**32**) with $HOCH_2CH_2OH$ failed.

Chart II

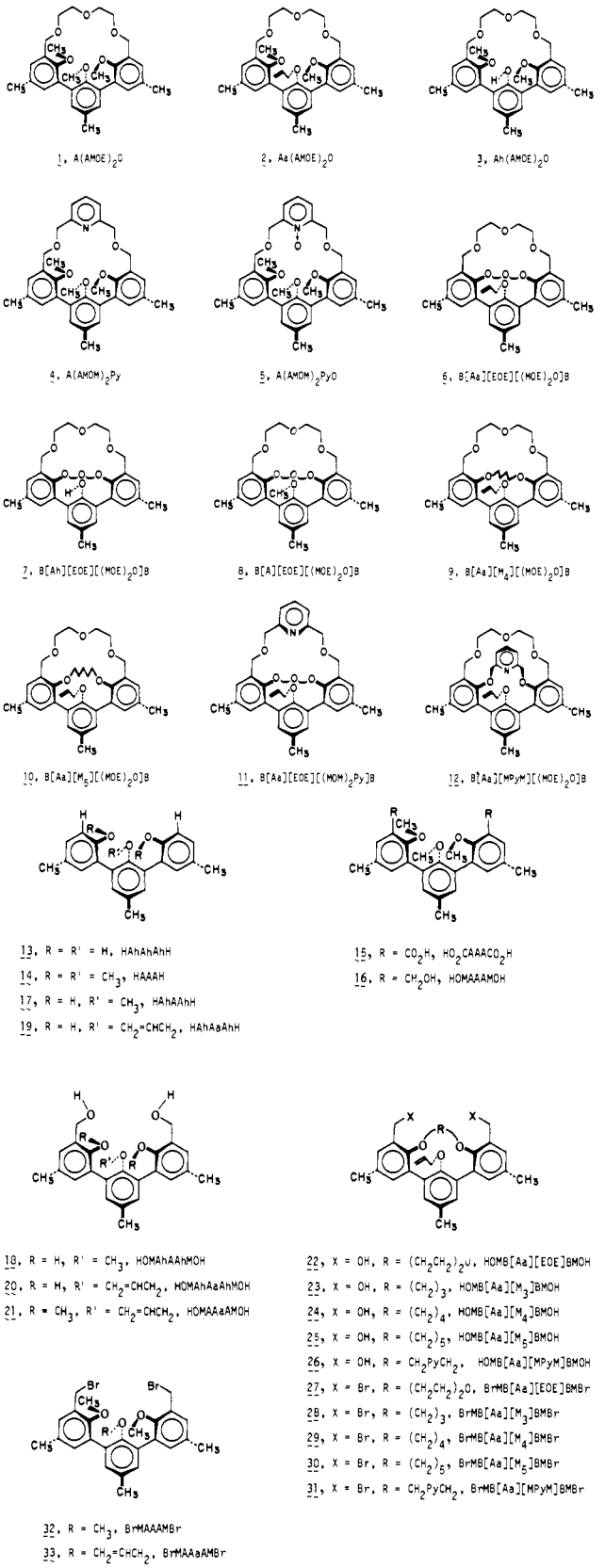

(4) Artz, S. P.; Cram, D. J. *J. Am. Chem. Soc.* **1984**, *106*, 2160–2171.
(5) Katz, H. E.; Cram, D. J. *J. Am. Chem. Soc.* **1984**, *106*, 4977–4987.
(6) Cram, D. J.; Dicker, I. B.; Lauer, M.; Knobler, C. B.; Trueblood, K. N. *J. Am. Chem. Soc.* **1984**, *106*, 7150–7167.
(7) Cram, D. J.; Trueblood, K. N. *Top. Curr. Chem.* **1981**, 43–106.
(8) Cram, D. J. "Proceedings of XVIII Solvay Conference in Chemistry on Design and Synthesis of Organic Molecules Based on Molecular Recognition", Wiley-Interscience: New York, in press.
(9) Newcomb, M.; Timko, J. M.; Walba, D. M.; Cram, D. J. *J. Am. Chem. Soc.* **1977**, *99*, 6392–6398.
(10) Baker, W.; Buggle, K. M.; McOmie, J. F. W.; Watkins, D. A. M. *J. Chem. Soc.* **1958**, 3594–3603.

Table I. Association Constants (K_a) and Binding Free Energies ($-\Delta G°$) of Hosts for Picrate Salts in $CDCl_3$ Saturated with D_2O at 25 °C

host structure	no.	Li^+	Na^+	K^+	Rb^+	Cs^+	NH_4^+	$CH_3NH_3^+$	t-$BuNH_3^+$	$-\Delta G°_{av}$[e]
				$-\Delta G°$[a] for Guest Cation, kcal mol^{-1}						
A(AMOE)$_2$O	**1**	7.0	12.2[b,c]	11.8[b,c]	10.4	9.0	9.9	8.2	7.7	9.5
Aa(AMOE)$_2$O	**2**	6.9	12.0[c]	11.3[c]	9.5	7.8	8.9	7.3	5.9	8.7
Ah(AMOE)$_2$O	**3**	6.5	7.9	8.0	6.8	6.5	6.4	5.9	4.1	7.3
A(AMOM)$_2$Py	**4**	7.4	12.0[c]	10.9[c]	9.0	7.8	8.7	7.4	6.3	8.7
B[Aa][EOE]-[(MOE)$_2$O]B	**6**	7.5	12.5[c]	12.9[c]	11.4	9.0	10.3	8.9	8.6	10.1
B[Ah][EOE]-[(MOE)$_2$O]B	**7**	6.8	8.9	10.2	8.4	7.4	8.2	6.6	6.5	7.9
B[A][EOE]-[(MOE)$_2$O]B	**8**	7.3	12.7[c]	13.9[c]	11.8[c]	9.7	11.1	9.9	8.9[c]	10.7
B[Aa][M$_4$]-[(MOE)$_2$O]B	**9**	5.7	10.3	8.7	6.5	5.8	6.7	4.9	~2.8	6.4
B[Aa][M$_5$]-[(MOE)$_2$O]B	**10**	5.7	8.7	9.1	6.8	5.8	6.7	4.6	~2.8	6.3
B[Aa][EOE]-[(MOM)$_2$Py]B	**11**	8.5	13.0[c]	12.2[c]	9.8	8.0	9.2	8.4	8.3	9.7
B[Aa][MPyM]-[(MOE)$_2$O]B	**12**	10.5	14.6[c]	14.6[c]	12.8[c]	11.3[c]	12.7[c]	11.9[c]	11.7[c]	12.5
Nap(OEOEO)$_2$E	**34**[d]	5.9	8.3	10.8	9.6	8.3	9.5	7.5	6.9	8.1
				K_a for Guest Cation, M^{-1}						
A(AMOE)$_2$O	**1**	1.3×10^5	9.2×10^8[b,c]	4.6×10^8[b,c]	4.6×10^7	3.7×10^6	1.5×10^7	9.9×10^5	4.2×10^5	5.2
Aa(AMOE)$_2$O	**2**	1.1×10^5	6.1×10^8[c]	2.0×10^8[c]	9.1×10^6	4.9×10^5	3.5×10^6	2.2×10^5	2.3×10^4	6.1
Ah(AMOE)$_2$O	**3**	6.0×10^4	6.3×10^5	7.2×10^5	9.8×10^4	6.2×10^4	4.9×10^4	2.2×10^4	9.4×10^2	3.9
A(AMOM)$_2$Py	**4**	2.6×10^5	6.1×10^8[c]	9.6×10^7[c]	4.0×10^6	5.3×10^5	2.2×10^6	2.6×10^5	3.9×10^3	5.7
B[Aa][EOE]-[(MOE)$_2$]O]B	**6**	3.2×10^5	1.4×10^9[c]	2.8×10^9[c]	2.2×10^8	4.0×10^6	3.5×10^7	3.4×10^6	2.8×10^6	5.4
B[Ah][EOE]-[(MOE)$_2$O]B	**7**	9.1×10^4	3.2×10^6	3.0×10^7	1.4×10^6	2.5×10^5	1.0×10^6	7.0×10^4	6.2×10^4	3.7
B[A][EOE]-[(MOE)$_2$O]B	**8**	2.2×10^5	2.1×10^9[c]	1.5×10^{10}[c]	4.4×10^8[c]	1.3×10^7	1.3×10^8	1.8×10^7	3.6×10^6	6.6
B[Aa][M$_4$]-[(MOE)$_2$O]B	**9**	1.6×10^4	3.6×10^7	2.5×10^6	5.8×10^4	1.9×10^4	7.5×10^4	4.0×10^3	$\sim 1.0 \times 10^2$	7.5
B[Aa][M$_5$]-[(MOE)$_2$O]B	**10**	1.5×10^4	2.5×10^6	4.6×10^6	9.5×10^4	1.7×10^4	7.5×10^4	2.4×10^3	$\sim 1.1 \times 10^2$	6.3
B[Aa][EOE]-[(MOM)$_2$Py]B	**11**	1.7×10^6	3.3×10^9[c]	8.6×10^8[c]	1.6×10^7	7.1×10^5	5.5×10^6	1.5×10^6	1.2×10^6	4.7
B[Aa][MPyM]-[(MOE)$_2$O]B	**12**	5.0×10^7	4.9×10^{10}[c]	4.9×10^{10}[c]	2.3×10^9[c]	1.9×10^8[c]	2.0×10^9[c]	5.0×10^8[c]	3.7×10^8[c]	4.1
Nap(OEOEO)$_2$E	**34**[d]	2.2×10^4	1.2×10^6	8.6×10^7	1.1×10^7	1.3×10^6	9.9×10^6	3.3×10^5	1.1×10^5	4.9

[a] All values obtained at $[H]_i \approx [G]_i \approx 0.015$ M and are averages of two determinations unless otherwise noted. [b] Values are average of four determinations. [c] Values were obtained at $[H]_i \approx [G] \approx 0.001$ M. [d] Values taken from ref 3. [e] In kcal mol^{-1}.

Likewise, the 16-membered host A(AMOM)$_2$M was not obtained from the reaction of $HOCH_2CH_2CH_2OH$ with BrMAAAMBr (**32**). Molecular models of A(AMO)$_2$E and A(AMOM)$_2$M can be made only by severely deforming the aromatic nuclei.

The yields in the final ring closures in making these hosts generally decrease as the systems become more crowded and tight. Molecular models (CPK) particularly of B[Aa][MPyM]-[(MOE)$_2$O]B (**12**) indicate it to be somewhat compressed and strained, and the yield was so low (4%) that it probably would not have been isolated had its t-$BuNH_3ClO_4$ complex not had good crystallizing properties. Models of B[Aa][M$_3$][(MOE)$_2$O]B, the compound we failed to isolate, also appear strained. In general, the yields of the bicyclic hosts are somewhat below those of the monocyclic compounds and decrease with the increase of strain that is visible in their CPK molecular models.

Macrocycles Aa(AMOE)$_2$O (**2**) and B[Aa][EOE]-[(MOE)$_2$O]B (**6**) were deallylated with PdC–EtOH–TsOH[11] to give phenolic hosts Ah(AMOE)$_2$O (**3**, 79%) and B[Ah]-[EOE][(MOE)$_2$O]B (**7**, 83%), respectively. Methylation of the latter compound with $(CH_3)_2SO_4$–NaOH–THF gave B[A]-[EOE][(MOE)$_2$O]B (**8**, 86%). Oxidation of A(AMOM)$_2$Py (**4**) with m-chloroperbenzoic acid in CH_2Cl_2 gave A(AMOM)$_2$PyO (**5**, 82%).

Determination of Association Constants and Free Energies of Binding. The association constants (K_a) and free energies of binding ($-\Delta G°$) of hosts **1–4**, **6–12**, and model chorand **34** in $CDCl_3$ saturated with D_2O at 25 °C were measured by the picrate extraction method.[12,13] Solutions of Li^+, Na^+, K^+, Rb^+, Cs^+, NH_4^+, $CH_3NH_3^+$, and t-$BuNH_3^+$ picrates in D_2O were extracted with $CDCl_3$ in the absence and presence of host. Control experiments established the fact that equilibrium was reached in <2 min of vortexing. The hosts and their complexes are soluble essentially only in the $CDCl_3$ layer. The Ka and $-\Delta G°$ values at 25 °C in $CDCl_3$ saturated with D_2O were calculated from the results and are recorded in Table I. Host A(AMOM)$_2$PyO (**5**) was found to provide binding free energies that were too low to be measured ($\Delta G°$ <6 kcal mol^{-1}).

When the initial concentrations of host and guest were 0.015 M and complexation was strong enough to provide ratios of complexed host at equilibrium to initial host (R values) of >0.9, small errors in R cause significant changes in K_a. This is true particularly for K_a values calculated from the amount of picrate ion in the organic phase, since at high R values, the calculations depend on small differences between large numbers. In such cases, the initial concentrations of host and guest were lowered to 0.001 M to bring R values into the sensitive range. In experiments at the lower concentration, 10 mL of each phase was employed except

(11) Boss, R.; Scheffold, R. *Angew. Chem., Int. Ed. Engl.* **1976**, *15*, 558–560.

(12) Helgeson, R. C.; Weisman, G. R.; Toner, J. L.; Tarnowski, T. L.; Chao, Y.; Mayer, J. M.; Cram, D. J. *J. Am. Chem. Soc.* **1979**, *101*, 4928–4941.

(13) Kaplan, L. J.; Weisman, G. R.; Cram, D. J. *J. Org. Chem.* **1979**, *44*, 2226–2233.

Table II. Selected Chemical Shifts of Protons in ^1H NMR Spectra (200 MHz, $CDCl_3$) of Macrocycles and Macrobicycles and Their Benzyl Bromide Precursors

	chemical shifts (δ)[a]				
compound	outer $ArCH_3$ (6 H)	inner $ArCH_3$ (3 H)	$OCH_2CH{=}CH_2$ (2 H)	inner OCH_3 (3 H)	$ArCH_2$ (4 H)
BrMAAAMBr (**32**)	2.328	2.370		3.190	4.625
A(AMOE)$_2$O (**1**)	2.319	2.454		2.563	4.402, 4.785
A(AMOM)$_2$Py (**4**)	2.350	2.391		2.686	
BrMAAaAMBr (**33**)	2.318	2.367	3.819		4.611
Aa(AMOE)$_2$O (**2**)	2.326	2.445	3.247		
BrMB[Aa][M$_3$]BMBr (**28**)	2.378	2.378	3.841		4.393, 4.895
BrMB[Aa][M$_4$]BMBr (**29**)	2.336	2.352			4.578
B[Aa][M$_4$][(MOE)$_2$O]B (**9**)	2.325	2.446			
BrMB[Aa][M$_5$]BMBr (**30**)	2.321	2.378	3.703		4.426, 4.810
B[Aa][M$_5$][(MOE)$_2$O]B (**10**)	2.321	2.442	3.266		
BrMB[Aa][EOE]BMBr (**27**)	2.329	2.391			4.385, 4.924
B[Aa][EOE][(MOE)$_2$O]B (**6**)	2.332	2.447	3.256		4.451, 4.676
B[Aa][EOE][(MOM)$_2$Py]B (**11**)	2.370	2.370	3.571		4.574, 5.094
BrMB[Aa][MPyM]BMBr (**31**)	2.324	1.997	4.215		4.675, 4.730
B[Aa][MPyM][(MOE)$_2$O]B (**12**)	2.326	2.260	3.211		

[a] Outer means groups flanking the plane of symmetry; inner means groups on the plane of symmetry.

Table III. Selected Chemical Shifts of Protons in ^1H NMR Spectra (200 MHz, $CDCl_3$) of Host A(AMOE)$_2$O (**1**) and B[A][EOE][(MOE)$_2$O]B (**8**) and Their Complexes

	chemical shifts (δ)[a]						
compound	outer $ArCH_3$ (6 H)	inner $ArCH_3$ (3 H)	outer OCH_3 (6 H)	inner OCH_3 (3 H)	outer Ar*H* (4 H)	inner Ar*H* (2 H)	$ArCH_2$[b] (4 H)
A(AMOE)$_2$O (**1**)	2.319	2.454	3.369	2.563	7.060, 7.077	7.251	4.402, 4.785
1·NaPic[c]	2.346	2.504	3.482	2.456	6.988, 7.152	7.330	3.913, 5.083
1·*t*-BuNH$_3$ClO$_4$[c]	2.324	2.498	3.524	2.196	7.028, 7.075	7.345	4.063, 5.140
B[A][EOE][(MOE)$_2$O]B (**8**)	2.326	2.452		2.586	7.092, 7.073	7.229	4.450, 4.723
8·NaPic[c]	2.352	2.495		2.470	7.035, 7.132	7.323	4.001, 5.195
8·KPic[c]	2.326	2.495		2.370		7.325	5.230

[a] Outer means groups flanking the plane of symmetry; inner means groups on the plane of symmetry. [b] AB quartet in the free cycle, and a doublet of doublets in the complexes. [c] One-to-one complex of host and guest.

with B[Aa][MPyM][(MOE)$_2$O]B (**12**) whose supply limited the volumes to 0.5 mL. Control experiments established that with care, the lower and higher volumes produced the same K_a and $-\Delta G°$ values. In all cases, K_a and $-\Delta G°$ values based on measurements in the D_2O and $CDCl_3$ layer were compared, and good agreement was observed when R values were <0.85. Table V of the supplementary material lists comparisons of R, K_a, and $-\Delta G°$ values based on measurements made in each phase at each of the two initial sets of concentration for those host–guest combinations that provided $-\Delta G°$ values in the 9–14 kcal mol^{-1} range. The K_a and $-\Delta G°$ values found in Table I are the average of the determination based on each phase in that concentration range which provided the most sensitive measurements. The values for Nap(OEOEO)$_2$E (**34**)[3] are included in Table for comparison purposes.

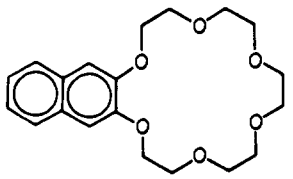

34, NAP(OEOEO)$_2$E

Chemical Shifts in ^1H NMR Spectra of Selected Hosts and Complexes. The hemispherands and their precursors are rich in aryl, arylmethyl, arylmethoxy, and arylmethylene groups whose proton chemical shifts provide clues as to the conformational organizations of the compounds as well as the structures of their complexes. Table II lists chemical shifts of selected protons in the ^1H NMR spectra of nonbridged and bridged dibromide intermediates and of the derived hosts. Table III provides chemical shifts of selected protons of A(AMOE)$_2$O (**1**) and several of its complexes as representative of a monocyclic host and of B[A]-[EOE][(MOE)$_2$O]B (**8**) and its complexes as representative of a bicyclic host. The relationships of these chemical shifts to structure will be discussed in the next sections.

Table IV. Distances (Å) and Angles in Crystal Structure of A(AMOE)$_2$O (**1**) and of A(AMOE)$_2$O·$(CH_3)_3CNH_3^+$

	A(AMOE)$_2$O	A(AMOE)$_2$O·$(CH_3)_3CNH_3^+$
distances between O's		
OCH_2CH_2O	3.61	2.89
$OArCH_2O$	3.58	3.08
inner–outer CH_3O's	3.56	3.98
outer–outer CH_3O's	2.84	2.83
distances O's are bent out of best plane of their attached aryls (av)	0.04	0.12
distances C's are bent out of best plane of their attached aryls (av)	0.10	0.28
angles of aryl fold around –O–Ar–CH_3 axis	2.5°	4.8°
Ar–Ar best plane dihedral angles (av)	58°	57°
angles between C—O—CH_3 plane and best aryl plane (av)	81°	80°
Ar–O–CH_3 bond angle (av)	115°	113°

Discussion

Crystal and Solution Structures of A(AMOE)$_2$O (1), Its Analogues, and Its Complexes. Views **35a** and **35b** of the crystal structure of A(AMOE)$_2$O (**1**)[14] and views **36a** and **36b** of the crystal structure of its complex A(AMOE)$_2$O·$(CH_3)_3CNH_3^+$ (**1**·*t*-BuNH$_3^+$)[7] are recorded in Chart I. Table IV lists the distances and angles of interest in these structures. Both views **35a** and **35b** of A(AMOE)$_2$O indicate that the AAA module is self-organized for binding during the synthesis but that the MOEOEOM bridge is not. Thus, in AAA the CH_3O groups

(14) Goldberg, I. *Cryst. Struct. Commun.* **1980**, *9*, 1201–1207.

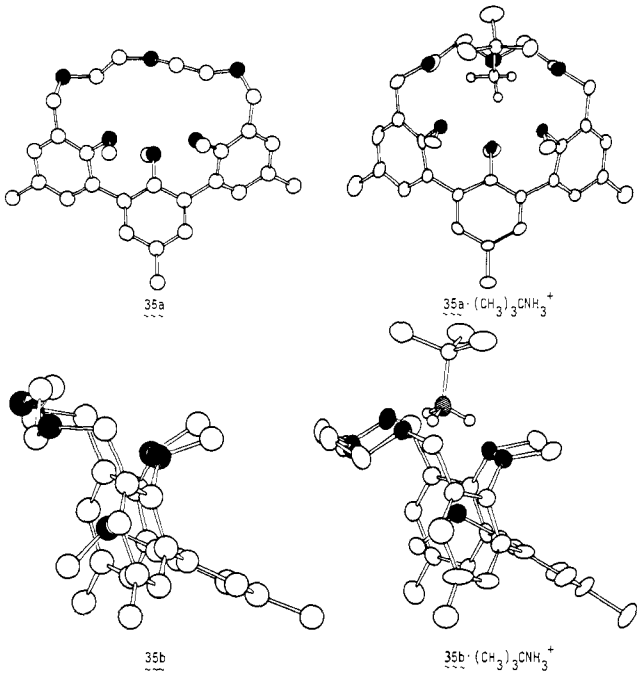

occupy an up–down–up position with the methyls diverging from the center and the orbitals of the unshared electron pairs of the oxygens converging on the center of the cavity. In the CH_2OC-$H_2CH_2OCH_2CH_2O$ bridge, the hydrogens of the most central CH_2 groups turn inward, filling the cavity, and the orbitals of the oxygen's unshared electron pairs diverge from the cavity in a nonbinding arrangement.

Upon complexation with $(CH_3)_3CNH_3^+$, the AAA module undergoes little reorganization while the MOEOEOM bridge undergoes extensive conformational change. In **35a**·$(CH_3)_3CNH_3^+$, the NH_3^+ group has displaced the inward-turned hydrogens of the CH_2 groups which now diverge from the cavity, bringing the orbitals of the unshared electron pairs of the oxygens into convergent alignments with the cavity to hydrogen bond the NH_3^+ group. The decreases in the distances between the oxygens of Table IV measure the extent of this reorganization. Thus, the OCH_2CH_2O distances decrease by 0.72 Å and the $OArCH_2O$ distances by 0.50 Å, whereas the inner–outer CH_3O oxygen distances increase by 0.42 Å and the outer–outer CH_3O oxygen distances remain the same in the complex as in the free host. In effect, the length of the MOEOEOM bridge shortens as *anti*-OCH_2CH_2O conformations become gauche. Thus, shortening *introduces strains* into the AAA module of three types: (1) The average distances that the oxygens are bent out of the best planes of their attached aryl groups increases by 0.08 Å. (2) The average distance that the carbons are bent out of the best planes of their attached aryls increases by 0.18 Å. (3) The average angles of fold of the three aryls around their O–Ar–CH_3 axis increases by 2.3°.

The complex is structured by three hydrogen bonds, two of the N–H···O types that involve the benzyl oxygens of the bridge and one that is bifurcated, N^+–H:::$(OCH_3)_2$. The bifurcated hydrogen bond involes the two outer methoxy oxygens whose positions do not change upon complexation. The four hydrogen-bonded oxygens are essentially coplanar, and the axis of the C–N bond of the guest is nearly normal to this plane. In the crystal structures of Nap(OEOEO)$_2$E·$(CH_3)_3CNH_3^+$ and other chorand complexes of RNH_3^+, the three hydrogen-bonded oxygens (tripod binding) define a plane, and the axis of the C–N bond of the guest is normal to this plane as well.[7] In both types of complexes as in others,[7] the H–N–C–C dihedral angles of the guest are about 60°.

The crystal structures observed for A(AMOE)$_2$O (**1**) and A(AMOE)$_2$O·$(CH_3)_3CNH_3^+$ are consistent with expectations based on CPK molecular model examination. Notice that the free host is "sided" in the sense that two outer methyl groups protrude upward and the inner methyl downward in **35a**, as in CPK molecular models. Models of two possible $(CH_3)_3CNH_3^+$ complexes of **1** can be constructed. The first resembles **35a** in which the guest perches on that side of the macroring from which *two methyls* protrude. This complex involves a tetrapod hydrogen bonding arrangement. In a second, the guest perches on the side of the macroring from which *one* methyl protrudes, whose attached oxygen acts as a binding site to provide *tripod* hydrogen bonding $N(H\cdots O)_3$. The latter structure appears less stable in models on three grounds: (1) The average O-to-N distance increases markedly in the tripod compared to the tetrapod structure. (2) The coplanarity of three benzene rings and their attached atoms are more compromised in the tripod than in the tetrapod structure. (3) The tetrapod structure is more compact and occupies a smaller hole in the solvent than the tripod structure. (4) The macroring must expand in the tripod structure beyond the size provided by the normal C–C–C bond angles, which is less true for the tetrapod structure. Thus, model examination suggests that the tetrapod structure should be more stable than the tripod structure of the complex.

The ^{1}H NMR spectral changes of A(AMOE)$_2$O (**1**) upon complexation with $(CH_3)_3CNH_3^+$ are consistent with the changes observed in the crystal structures of A(AMOE)$_2$O when it complexes with $(CH_3)_3CNH_3^+$ (Table III). The chemical shift changes of the nine CH_3Ar and six ArH protons in passing from free host to complex in solution range only from 0.002 to 0.032 ppm, which correlates with the lack of change in the Ar–Ar dihedral angle upon complexation in the crystal (Table IV). Complexation causes much greater chemical shifts that range from 0.16 to 0.37 ppm for the nine CH_3O and four $ArCH_2$ protons, which correlates with the lowered conformational mobility of these groups in the complex vs. in the free host. The chemical shift of the inner CH_3O protons moves upfield by successive stages in passing from BrMAAAMBr (**32**, δ 3.190) to A(AMOE)$_2$O (**1**, δ 2.563) to A(AMOE)$_2$O·*t*-$BuNH_3^+$ (δ 2.196). A comparison of the molecular models of these species indicates that the inner OCH_3 protons move ever more deeply into the shielding region of the three aryl groups as the two ends of the AAA module are forced closer, first by their becoming part of a ring and then by the complexing act itself.

The chemical shift pattern of the outer CH_3O protons is entirely different. Their chemical shifts start much further downfield in BrMAAAMBr (**32**, δ 3.560), move upfield in A(AMOE)$_2$O (**1**, δ 3.369), but downfield again in A(AMOE)$_2$·*t*-$BuNH_3^+$ (δ 3.524). Model examination of these species indicates that cyclization conformationally confines the outer CH_3O protons to the shielding region of its two closest aryls. Upon complexation, the methoxy methyls turn away from the central aryl ring to focus the electron pairs of their attached oxygens on the NH^+ of the guest, and therefore they are less shielded and more downfield.

The $ArCH_2$ protons in BrMAAAMBr (**32**) occur as a singlet at δ 4.625 since they rapidly equilibrate on the ^{1}H NMR time scale. Upon cyclization to A(AMOE)$_2$O (**1**) they become an AB quartet, with one proton moving upfield to δ 4.402 and the other downfield to δ 4.785, whereas in A(AMOE)$_2$O·*t*-$BuNH_3^+$ they more further to δ 4.063 and 5.083. Both models and the crystal structures suggest that the upfield proton shares that face of the macroring with the two upward turned methyls and is much more in the shielding cone of its attached aryl group than the downfield proton, which lies closer to the plane of its attached aryl. The effect is more pronounced in the more rigid complex than in the more conformationally mobile host, as expected.

The trends of chemical shift movements upon complexation observed for formation of A(AMOE)$_2$O·*t*-$BuNH_3^+$ carry over to A(AMOE)$_2$O·Na^+. Furthermore, both the values and the patterns of chemical shifts of host A(AMOE)$_2$O (**1**) and its complexes are similar to the much more rigid bicyclic host B[A][EOE]-[(MOE)$_2$O]B (**8**) and its complexes (see Table III). Thus, the monocyclic and bicyclic hosts and their complexes appear similarly organized in solution, although the bicyclic system must be less conformationally mobile. The patterns of chemical shifts for the other dibromides, macrocycles, and macrobicycles listed in Table II provide no surprises. The hosts appear to be similarly organized

with varying degrees of rigidity, depending on the length and character of the centrally drawn bridges in formulas **2**, **4**, **6**, and **9–12**.

Correlation of Binding Free Energy with Structure. This and other studies have led us to design hot–guest relationships and to interpret complexation free energies in terms of two self-evident guiding principles. The *principle of complementarity* points to the expectation that to complex, hosts must have binding sites which cooperatively contact and attract the binding sites of guests without generating strong nonbonded repulsions. The *principle of preorganization* states that the smaller the changes in organization of hosts and guests required for complexation, the stronger the binding.[4] Structural recognition depends on both complementarity and preorganization and is measured by the differences in free energies of complexation between possible complexing partners and each complexing separately with their solvent shells.[4] The $-\Delta G°$ alues of Table I vary from a high of 14.6 kcal mol^{-1} to a low of ~2.8 kcal mol^{-1}. The general binding ability of each host is characterized by its $-\Delta G°_{av}$ value, whereas its $\Delta(\Delta G°)_{max}$ value measures its general ability to distinguish between guests. The $-\Delta G°_{av}$ values range from a high of 12.5 kcal mol^{-1} to a low of 6.3 kcal mol^{-1}. The hosts rank in decreasing order as general complexing partners as follows: B[Aa][MPyM][$(MOE)_2$O]B (**12**) > B[A][EOE][$(MOE)_2$O]B (**8**) > B[Aa][EOE][$(MOE)_2$O]B (**6**) > B[Aa][EOE][$(MOM)_2$Py]B (**11**) > A$(AMOE)_2$O (**1**) > Aa$(AMOE)_2$O (**2**) ≡ A$(AMOE)_2$Py (**4**) > Nap$(OEOEO)_2$E (**34**) > B[Ah][EOE][$(MOE)_2$O]B (**7**) > Ah$(AMOE)_2$O (**3**) > B[Aa][M_4][$(MOE)_2$O]B (**9**) ~ B[Aa][M_5][$(MOE)_2$O]B (**10**).

More specific comparisons identify those structural features that enhance or depress general complexing power. The three nonbridged compounds (**1**, **2**, and **4**) are better binds than chorand Nap$(OEOEO)_2$E (**34**) by an average value of almost 1 kcal mol^{-1}. We attribute this to the self-organizing ability of three anisyl groups whose up–down–up binding conformations are fixed during synthesis rather than during the complexing act. Although the MOEOEOM modules of **1**, **2**, and **4** need to be conformationally reorganized during complexation, fewer degrees of freedom need to be frozen out than in chorand **34**. The effect would be even greater than observed were it not for the increased strain introduced into the hemispherand hosts during complexation. This strain is associated with the greater deformation of the aryls and their attached atoms from planarity (see Table IV).

Introduction of additional bridges into the hemispherands greatly rigidifies them, increasing or depressing their binding power according to the degree to which the binding sites are directed toward or away from the geometry needed for complexing. In hosts B[Aa][MPyM][$(MOE)_2$O]B (**12**), B[Aa][EOE][$(MOE)_2$O]B (**8**), B[Aa][EOE][$(MOE)_2$O]B (**6**), and B[Aa][EOE][$(MOM)_2$Py]B (**11**), the additional bridges each contain an additional binding site, which in molecular models appears roughly held in a binding conformation. The MPyM bridge in B[Aa][MPyM][$(MOE)_2$O]B (**12**) imparts the highest degree of preorganization for binding in molecular models and the highest observed $-\Delta G°_{av}$ value of 12.5 kcal mol^{-1}. Part of the preorganization in **6**, **8**, **11**, and **12** involves steric inhibition of solvation of the binding sites of the host by H_2O or $CHCl_3$. In their models, their binding sites are better insulated from solvation by the increased number of hydrocarbon groups oriented toward their surfaces. Another aspect of the preorganization of **6**, **8**, **11**, and **12** is that their extra bridges tend to fix the lengths of, and limit the conformations available to, the MOEOEOM module. Thus, upon complexation, fewer conformations need to be frozen out and less strain needs to be introduced into the preorganized BAB parts of the host than with A$(AMOE)_2$O (**1**). In other words, the free energy bill for conformationally organizing and desolvating these bicyclic hosts is more fully paid during their syntheses than with the monocyclic hosts (principle of preorganization).

In contrast to the extra bridges in **6**, **8**, **11**, and **12**, the M_4 and M_5 bridges of B[Aa][M_4][$(MOE)_2$O]B (**9**) and B[Aa][M_5][$(MOE)_2$O]B (**10**) do not contain extra binding sites. Those bridges in molecular models do inhibit solvation of both the hosts themselves and of their complexes. The M_4 bridge also rigidifies B[Aa][M_4][$(MOE)_2$O]B (**9**) in the direction of limiting its cavity size, making it a much poorer binder of the larger ions than Nap$(OEOEO)_2$E (**34**) but a better binder of Na^+ by 2 kcal mol^{-1} than Nap$(OEOEO)_2$E. The longer M_5 bridge in models of B[Aa][M_5][$(MOE)_2$O]B (**10**) provides the bicyclic ring system with a potentially larger cavity but also with many more nonbinding conformations that need to be frozen out during complexation. These effects provide a peak binding by **10** for K^+ ion of 9.1 kcal mol^{-1}, 1.7 kcal mol^{-1} less than the 10.4 kcal mol^{-1} observed for Nap$(OEOEO)_2$E. Both the M_4 and M_5 bridges have a net inhibitory effect on binding. This conclusion derives from the fact that Aa$(AMOE)_2$O (**2**) without an extra bridge binds Na^+ and K^+ ions with $-\Delta G°$ values of 12.0 and 11.3 kcal mol^{-1}, respectively, which substantially exceeds the values of 10.3 and 8.7 for Na^+ and 8.7 and 9.1 for K^+ ions observed for B[Aa][M_4][$(MOE)_2$O]B (**9**) and B[Aa][M_5][$(MOE)_2$O]B (**10**), respectively.

Substitution of the more rigid MPyM for the EOE unit can either inhibit or enhance binding, depending on wehter the longer or shorter bridge of the host is involved. Thus, A$(AMOE)_2$O (**1**) has a $-\Delta G°_{av}$ value 1.8 kcal mol^{-1} greater than that of A$(AMOM)_2$Py (**4**), and B[Aa][EOE][$(MOE)_2$O]B (**6**) has a $-\Delta G°_{av}$ value 0.4 kcal mol^{-1} greater than that of B[Aa][EOE][$(MOM)_2$Py]B (**11**). However, B[Aa][MPyM][$(MOE)_2$O]B (**12**) has a $-\Delta G°_{av}$ value 2.4 kcal mol^{-1} higher than B[Aa][EOE][$(MOE)_2$O]B (**6**). These results probably represent the superposition of opposing effects. Ether oxygens have two sets of unshared pairs available for ligating compared to one pair for pyridine, and, therefore, less specific orientation is needed for binding by an EOE than by a MPyM unit. However, the EOE unit is more conformationally mobile than the MPyM unit. The fact that A$(AMOM)_2$PyO (**5**) turned out not to complex well enough to be even "on scale" appears to be associated with the placement of oxygen of the pyridine oxide. In molecular models of **5**, the PyO oxygen occupies the position normally occupied by the guest in the complexes.

The hemispherands contain the three kinds of inner aryloxy units, A, Aa, and Ah. Of these, the A unit (p-$CH_3C_6H_2OCH_3$) provides the strongest binding, the Aa (p-$CH_3C_6H_2OCH_2CH{=}CH_2$) unit the next, and the Ah(p-$CH_3C_6H_2OH$) unit the weakest binding. For example, $-\Delta G°_{av}$ values for A$(AMOE)_2$O (**1**), Aa$(AMOE)_2$O (**2**), and Ah$(AMOE)_2$O (**3**) are 9.5, 8.7, and 7.3 kcal mol^{-1}, respectively. Likewise the values ofr B[A][EOE][$(MOM)_2$O]B (**8**), B[Aa][EOE][$(MOM)_2$O]B (**6**), and B[Ah][EOE][$(MOM)_2$O]B (**7**) are 10.7, 10.1, and 7.9 kcal mol^{-1}, respectively. The electron-withdrawing inductive effect of the vinyl group in Aa vs. the hydrogen of A may be responsible for A being a better ligand than Aa. The average loss in binding of 2.5 ± 0.3 kcal mol^{-1} in passing from A to the Ah group very likely is due to intramolecular hydrogen bonding of the OH of the Ah group to neighboring oxygens in the free host. This hydrogen bond must be broken upon complexation, whose cost comes out of the binding free energy.

Structural Recognition in Host–Guest Complexation. The major ring system in these hemispherands is 18-membered, and they tend to show peak binding with Na^+ and K^+ as guests. Because of the importance of Li^+, Na^+, K^+, and NH_4^+ in physiological chemistry, the ability of hosts to differentiate between these ions in complexation is interesting. Also of interest are the relationships between general binding ability, specificity, and structure. If $-\Delta(\Delta G°)_{max}$ is used as a *general indicator* of specificity, the hosts rank in the following order: B[Aa][M_4][$(MOE)_2$O]B (**9**, 7.5 kcal mol^{-1}) > B[A][EOE][$(MOE_2O]$B (**8**, 6.6) > B[Aa][M_5][$(MOE)_2$O]B (**10**, 6.3) > Aa$(AMOE)_2$O (**2**, 6.1) > A$(AMOM)_2$Py (**4**, 5.7) > B[Aa][EOE][$(MOE)_2$O]B (**6**, 5.4) > A$(AMOE)_2$O (**1**, 5.2) > Nap$(OEOEO)_2$E (**34**, 4.9) > B[Aa][EOE][$(MOM)_2$Py]B (**11**, 4.7) > B[Aa][MPyM][$(MOE)_2$O]B (**12**, 4.1) > Ah$(AMOE)_2$O (**3**, 3.9) > B[Ah][EOE][$(MOE)_2$O]B (**7**, 3.7 kcal mol^{-1}). If the internally hydrogen-bonded hosts **3** and **7** and B[A][EOE][$(MOE)_2$O]B (**8**) are disregarded, there is a near inverse order for general binding ability as measured by $-(\Delta G°)_{av}$ and structured recognition as measured by $-\Delta(\Delta G°)_{max}$. Particularly striking are the inverse positions occupied in the order

by B[Aa][MPyM][$(MOE)_2O$]B (**12**) and by B[Aa][M_4]-[$(MOE)_2O$]B (**9**). Thus, **12** is the best general but one of the least discriminate binders, and **9** is the most discriminating but almost the least good general complexing host. Both hosts are among the most rigidly structured of the series. Clearly general specificity, general binding, and structural rigidity do not correlate in this series of compounds.

More narrow correlations of specificity with structure are measured by $K_a^G/K_a^{G'}$ ratios, where G and G′ are guest ions adjacent to one another in the ionic diameter orders (alkali-metal ions) or degrees of substitution (ammonium and alkylammonium ions). None of the hosts bind Li^+ better than Na^+. The highest $K_a^{Na^+}/K_a^{Li^+}$ values are provided by B[A][EOE][$(MOE)_2O$]B (**8**, ratio of 9500) and A$(AMOE)_2O$ (**1**, ratio of 7100). The highest $K_a^{Na^+}/K_a^{K^+}$ values are found with B[Aa][M_4][$(MOE_2O]$B (**9**, ratio of 14) and A$(AMOM)_2$Py (**4**, ratio of 6). The highest $K_a^{K^+}/K_a^{Na^+}$ values are observed with Nap$(OEOEO)_2$E (**34**, ratio of 72) and B[Ah][EOE][$(MOE)_2O$]B (**7**, ratio of 9). The highest K^{K^+}/K^{Rb^+} values are found with B[Aa][EOE][$(MOM)_2$Py]B (**11**, 54) and B[Aa][M_5][$(MOE)_2O$]B (**10**, ratio of 48). None of the hosts binds Rb^+ better than K^+. The highest K^{Rb^+}/K^{Cs^+} values are found with B[Aa][EOE][$(MOE)_2O$]B (**6**, ratio of 55) and B[A]-[EOE][$(MOE)_2O$]B (**8**, ratio of 34). None of the hosts binds Cs^+ better than Rb^+. The highest $K^{NH_4^+}/K^{CH_3NH_3^+}$ value is observed with B[Aa][M_5][$(MOE)_2O$]B (**10**, ratio of 31). The highest $K^{CH_3NH_3^+}/K^{t\text{-}BuNH_3^+}$ value is provided by B[Aa][M_4][$(MOE)_2O$]B (**10**, ratio of 40). As has been observed for other systems,[4] the K_a values for Rb^+ and NH_4^+ tend to favor Rb^+ but tend to be very close to one another for all hosts, the biggest difference being $K_a^{Rb^+}/K_a^{NH_4^+} = 6$ for B[Aa][EOE][$(MOE)_2O$]B (**6**).

Trends in Binding Free Energies Potentially Useful in Designing Structural Recognition into Hosts. Table I provides data potentially useful in selecting binding units or modules which by their combinations in the same host might enhance binding specificity of one ion over another. For example, an examination of the column of $-\Delta G°$ values for Li^+ indicates that hosts in which a MPyM module replaces EOE, the $-\Delta G°$ values increase by 0.3 to 3 kcal mol^{-1}. This trend is less marked or absent in the columns for the other ions. Possibly lithium-specific hosts should be rich in MPyM modules. This reasoning suggests that B[Aa]-[MPyM][$(MOM)_2$Py]B might bind Li^+ either comparably or better than Na^+, a hypothesis suggested also by molecular model examination. Unfortunately, the compound resisted our attempts at its synthesis. Its models are more strained and more rigid than those of B[Aa][MPyM][$(MOE)_2O$]B (**12**).

Suppose specificity for Na^+ over K^+ binding by a host is desired. Comparisons of the binding patterns of **1** with **2** and of **6** with **8** suggest that substitution of Aa for A units tend to favor Na^+ over K^+. Comparisons of the binding patterns of **1** with **4** and of **6** with **11** suggest that substitution of MPyM for EOE modules in the central ring tend to favor Na^+ over K^+ binding. Comparisons of binding patterns of **6** with **9** suggest that substitution of M_4 for EOE modules in the minor bridge tend to favor Na^+ over K^+. When these modules or units that favor Na^+ are combined in the same compounds, potential host B[Aa][M_4]-[$(MOM)_2$Py]B results, which has not been prepared. A molecular model of this compound also suggests that Na^+ should be substantially favored over K^+.

Presume that specificity of K^+ over Na^+ binding is a desired property. Comparisons of the Na^+ and K^+ columns of $-\Delta G°$ values of Table I reveal that substitution of Ah for Aa or A units, EOE for MPyM modules, and M_5 for M_4 or EOE modules should favor K^+ over Na^+ binding. Possibly the host most likely to show the desired specificity would be B[Ah][M_5][$(MOM)_2O$]B.

These kinds of analyses assume additivity of free energy contributions of units or modules to the total binding free energy that a host has for a particular guest. Reasoning by analogy in this way is most likely to work in very closely related systems in which the major ring size and degrees of rigidity are not widely varied.

Special Character of B[Aa][MPyM][$(MOE)_2O$]B (12). This host is unusual in the sense that of the ligand systems reported here, it most strongly binds *each of* the eight guests. Values of $-\Delta G°$ range from 10.5 to 14.6 kcal mol^{-1} for **12** binding the alkali-metal ions. In molecular models, it is the host of this series most rigidly preorganized for binding. The orbitals of the unshared electron pairs in the four closely packed binding sites of the least strained conformation of the B[Aa][MPyM]B moiety all converge to form a partial cavity complementary to ions of those diameters studied here. Lithium ion with a diameter of 1.3–1.7 Å[15] can partially nest in this partial cavity, whereas Cs^+ with a diameter of about 3.2 Å must perch on the four sites. There are essentially no conformational degrees of freedom in the B[Aa][MPyM]B assembly, once the OEOEO bridge is in place, as in **12**. In models of **12**, the benzene ring of the Aa unit and the Py unit contact one another and lie in nearly parallel planes. The CH_2 hydrogens of the $CH_2CH{=}CH_2$ group in the Aa unit are rigidly held in the shielding cones of the Aa and two B units, which accounts for the marked movement upfield of the chemical shift of these hydrogens to δ 3.211 in the ^1H NMR spectrum of **12**. These hydrogens occur at δ 4.215 in the spectrum of BrM[Aa][MPyM]BMBr.

The length of the MOEOEOM bridge in models of B[Aa]-[MPyM][$(MOE)_2O$]B (**12**) is essentially limited to its most extended forms in both the free host and its complexes by the rigidity of the B[Aa][MPyM]B module. Thus, the strain in this module is introduced during the synthesis of **12**, rather than during the complexation as in A$(AMOE)_2O$ (**1**, see Table IV). In concert with this interpretation, the yield in the final ring closure of **12** was only ~5%. The limited length of the MOEOEOM bridge in **12** imposes on it conformational constraints which clearly favor locating the central oxygen of the bridge directly above the four binding sites of the B[Aa][MPyM]B module. The orbitals of the unshared electron pairs of this central oxygen converge on the four-atom partial nest. The resulting five binding sites are beautifully complementary to spheres that range from about 1.4 to 2.5 Å in diameter. Conformations are available to the MOEOEOM bridge which also focus the orbitals of the unshared electron pairs of the two benzyl oxygens on the center of the cavity. In such conformations, the cavity diameter is complementary to spheres of diameters that range from about 2.5 to 3.4 Å. Thus, the high binding free energies of all of the alkali-metal ions are accounted for.

Equally striking are the $-\Delta G°$ values that **12** exhibits toward NH_4^+ (12.7), $CH_3NH_3^+$ (11.9), and t-$BuNH_3^+$ (11.7 kcal mol^{-1}). In models of **12**·NH_4^+, there are four linear (tetrahedrally arranged) hydrogen bonds. The oxygen of the Aa unit, the nitrogen of the NH_4^+, and the nitrogen of the Py group define one plane, perpendicular to which is another plane defined by the two benzyl oxygens and the NH_4^+ nitrogen. The central oxygen of the MOEOEOM bridge and the two oxygens of the two B groups also each contact two hydrogens of the NH_4^+ guest in between the hydrogen bonds to form a wonderfully compact structure in which all seven binding sites of the host are occupied. The similar but less perfectly tailored models of tetrapodal complexes of B-[Aa][EOE][$(MOE)_2O$]B·NH_4^+ (**6**·NH_4^+) and B[A][EOE]-[$(MOE)_2O$]B·NH_4^+ (**8**·NH_4^+) account for the high values of 10.3 and 11.1 kcal mol^{-1} binding observed for **6** and **8** complexing NH_4^+, respectively.

In models of **12**·$CH_3NH_3^+$ and **12**·t-$BuNH_3^+$, the Py and two benzyl oxygens form linear hydrogen bonds in a tripod arrangement, while the EOE and the two oxygens of the B units occupy the three "in-between positions", each contacting two of the NH hydrogens. The oxygen of the Aa group contacts the N^+ in between the three hydrogen bonds, 180° from the C–N bond of the guest. Thus, four of the binding sites of **12** are rigidly preorganized for complexation, whereas the other three have very limited degrees of freedom, but which can wonderfully adapt to all eight guests of this study.

Registry No. 1, 73522-93-7; **1**·t-$BuNH_3ClO_4$, 93645-18-2; **1**·NaPic, 93645-17-1; **2**, 93683-23-9; **3**, 93645-01-3; **4**, 83632-47-7; **5**, 93645-02-4; **6**, 82484-57-9; **7**, 83587-09-1; **8**, 82475-15-8; **8**·NaPic, 93645-19-3; **8**·KPic, 93645-21-7; **9**, 93645-03-5; **10**, 87199-23-3; **11**, 93645-04-6; **12**,

(15) Trueblood, K. N.; Knobler, C. B.; Maverick, E.; Helgeson, R. C.; Brown, S. B.; Cram, D. J. *J. Am. Chem. Soc.* **1981**, *103*, 5594–5596.

93645-05-7; **12**·*t*-$BuNH_3ClO_4$, 93683-26-2; **13**, 71128-89-7; **16**, 71128-92-2; **17**, 73229-34-2; **18**, 93645-06-8; **19**, 83587-06-8; **20**, 83587-07-9; **21**, 93683-24-0; **22**, 83603-87-6; **23**, 93683-25-1; **24**, 93645-07-9; **25**, 93645-08-0; **26**, 93645-09-1; **27**, 83587-08-0; **28**, 93645-10-4; **29**, 93645-11-5; **30**, 93645-12-6; **31**, 93645-13-7; **32**, 71128-93-3; **33**, 93647-14-8; **34**, 17454-52-3; CH_2=$CHCH_2Br$, 106-95-6; $Br(CH_2)_4Br$, 110-52-1; $Br(CH_2)_5Br$, 111-24-0; $Br(CH_2)_3Br$, 109-64-8; *t*-$BuNH_3ClO_4$, 18720-49-5; Li^+, 17341-24-1; Na^+, 17341-25-2; K^+, 24203-36-9; Rb^+, 22537-38-8; Cs^+, 18459-37-5; NH_4^+, 14798-03-9; $CH_3NH_3^+$, 17000-00-9; *t*-$BuNH_3^+$, 22534-19-6; 3-(hydroxymethyl)-2′-[(2-propen-1-yl)-oxy]-5,5′,5″-trimethyl[1,1′:3′,1″]terphenyl-2,2″-diol, 93645-15-9; diethyleneglycol ditosylate, 7460-84-2; 2′-hydroxy-2,2″-dimethoxy-3,3″-bis(bromomethyl)-5,5′,5″-trimethyl[1,1′:3′,1″]terphenyl, 93645-16-0; diethyleneglycol, 111-46-6; pyridine-2,6-dimethanol, 1195-59-1; 2,6-bis(bromomethyl)pyridine, 7703-74-4.

Supplementary Material Available: Experimental procedures for the syntheses of compounds **2–33**, their systematic names, characterization, and a modified method for determining K_a and $-\Delta G°$ values at more dilute concentrations (24 pages). Ordering information is given on any current masthead page.

Observation of Transient Cyclohexadienones during the Aqueous Bromination of Phenols. Mechanisms of Enolization

Oswald S. Tee* and N. Rani Iyengar

Contribution from the Department of Chemistry, Concordia University, 1455 de Maisonneuve Quest, Montrêal, Québec, Canada H3G 1M8. *Received August 14, 1984*

Abstract: Transient 4-bromo-2,5-cyclohexadienone intermediates have been observed during the aqueous bromination of phenol and several methylated derivatives. They enolize to the corresponding *p*-bromophenols by both acid-catalyzed and water-catalyzed pathways in the pH range 0–6. Studies carried out in buffers also indicate both general acid catalysis ($\alpha \simeq 0.0$) and general base catalysis ($\beta = 0.54$). The latter is ascribed to simple rate-limiting proton abstraction, but the former is not so easily rationalized. The very low α is attributed to a termolecular transition state (water, substrate, and general acid) in which the dienone becomes more *anion-like* than cation-like. This seemingly anomalous behavior can be explained by the very large enol/keto ratio ($\sim 10^{11}$) for phenol.

Various evidence points to the intermediacy of cyclohexadienones in the electrophilic bromination of phenols (eq 1).[1] In particular, Ershov and Volod'kin isolated the dienone **2g** from the reaction of bromine with 2,6-di-*tert*-butylphenol in acetic acid.[2] Subsequently, its behavior in acetic acid was extensively studied by de la Mare and co-workers.[1b] Using flow NMR methods, Fyfe and Van Veen observed several such dienones formed from 2,6-dialkylphenols and bromine, also in acetic acid.[3]

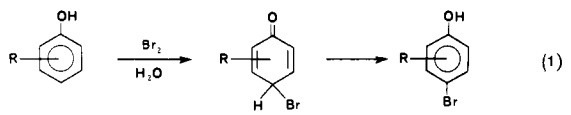

(1)

1 2 3

a, parent; b, R = 2-Me; c, R = 3-Me; d, R = 2,6-Me_2; e, R = 3,5-Me_2; f, R = 2,5-Me_2; g, R = 2,6-(*t*-Bu)$_2$

We recently reported that transient 4-bromo-2,5-cyclohexadienones (**2**) can be observed during the aqueous bromination of simple phenols.[4] This ability allows, for the first time, a detailed study of the enolization of such dienones in aqueous solution, and such is the subject of the present paper. We have found general acid and general base catalysis, as one might expect by analogy with the enolization of simple ketones.[5] However, the general acid catalysis observed cannot be explained by simple rate-limiting proton transfer from a general acid or by specific/general base catalysis.

Results

We have observed the transient dienones **2a–f** derived from phenol and various methyl derivatives (**1a–f**).[6] We have failed to detect any cyclohexadienones derived from phenols bearing electron-withdrawing groups (see Discussion).

Table I. Rate Constants for the Enolization of 4-Bromo-2,5-cyclohexadienones (**2**) in Aqueous Acidic Solution;[a] See Equation 2

dienone (**2**)	pK_a of **1**[b]	k_0, s^{-1}	k_H, M^{-1} s^{-1}
parent (**2a**)	9.95	16.1	111
2-methyl (**2b**)	10.28	3.22	48.2
3-methyl (**2c**)	10.08	9.98	36.1
2,6-dimethyl (**2d**)	10.63	0.572[c]	3.17
3,5-dimethyl (**2e**)	10.19	4.81	1190
2,5-dimethyl (**2f**)	10.41	2.41	169

[a] At 25 °C, I = 0.1 M (KBr). [b] From: Jencks, W. P.; Regenstein, J. In "Handbook of Biochemistry and Molecular Biology", 3rd ed.; Fasman, G. D., Ed.; CRC Press: Cleveland, Ohio, 1976; Vol. I, p 314. [c] The average value obtained from the intercepts of buffer plots (I = 1.0 M) is 0.425 s^{-1}.

While measuring the rate of bromination of phenol at 265 nm (tribromide ion band), as is customary,[7] we noted that the final absorbance value tailed downward slightly. However, when the reaction was followed at 275 nm no such tailing was apparent (Figure 1). Furthermore, at 235–240 nm we observed a trace (Figure 1) appropriate to the first-order formation and decay of a transient intermediate.[8,9] The rate of the increase matches the decrease at 275 nm, and it is proportional to the phenol concentration.[10] The extent of the increase at 237 nm varies in proportion

(1) (a) de la Mare, P. B. D. "Electrophilic Halogenation"; Cambridge University Press: Cambridge, England, 1976. (b) de la Mare, P. B. D. *Acc. Chem. Res.* **1974**, *7*, 361 and references therein.
(2) Ershov, V. V.; Volod'kin, A. A. *Izv. Akad. Nauk. SSSR, Otd. Khim. Nauk.* **1962**, 730; *Chem. Abstr.* **1962**, *57*, 12337c.
(3) Fyfe, C. A.; Van Veen, L., Jr. *J. Am. Chem. Soc.* **1977**, *99*, 3366.
(4) Tee, O. S.; Iyengar, N. R.; Paventi, M. *J. Org. Chem.* **1983**, *48*, 759.
(5) Toullec, J. *Adv. Phys. Org. Chem.* **1982**, *18*, 1 and references therein.
(6) Dienones arising from ipso bromine attack on *p*-cresol[4] and other *p*-alkyl phenols have also been detected in this laboratory. Their decomposition, which does not involve enolization,[4] is being studied separately.
(7) (a) Tee, O. S.; Berks, C. G. *J. Org. Chem.* **1980**, *45*, 830. (b) Tee, O. S.; Paventi, M. *J. Am. Chem. Soc.* **1982**, *104*, 4142. (c) Tee, O. S.; Thackray, D. C.; Berks, C. G. *Can. J. Chem.* **1978**, *56*, 2970.
(8) Moore, J. W.; Pearson, R. G. "Kinetics and Mechanism"; Wiley: New York, 1981; p 290.
(9) The 237-nm trace in Figure 1 can be computer simulated by using the appropriate equation from ref 8 with rate constants of 68 and 14 s^{-1} and an apparent extinction coefficient for the intermediate of 8900.

0002-7863/85/1507-0455$01.50/0